



**Control of co-existing phases and charge transport in a nanostructured manganite film by field effect with an electric double layer as the gate dielectric**

Journal:	<i>RSC Advances</i>
Manuscript ID:	RA-ART-05-2015-009081.R1
Article Type:	Paper
Date Submitted by the Author:	09-Jun-2015
Complete List of Authors:	NATH, RAJIB; S. N. Bose National Centre for Basic Sciences, Condensed Matter Physics & Material Sciences Raychaudhuri, Arup; S. N. Bose National Centre for Basic Sciences,, Condensed Matter Physics & Material Sciences

# Control of co-existing phases and charge transport in a nanostructured manganite film by field effect with an electric double layer as the gate dielectric

Rajib Nath,<sup>\*a</sup> and A. K. Raychaudhuri<sup>a</sup>

Received Xth XXXXXXXXXXXX 20XX, Accepted Xth XXXXXXXXXXXX 20XX

First published on the web Xth XXXXXXXXXXXX 200X

DOI: 10.1039/b000000x

We report a bipolar control of co-existing phases in a nanostructured film of manganite  $\text{La}_{0.85}\text{Ca}_{0.15}\text{MnO}_3$ , using an applied gate bias in a field effect (FE) device configuration. Low hole-doped manganite  $\text{La}_{0.85}\text{Ca}_{0.15}\text{MnO}_3$  shows the co-existence of different electronic phases and a ferromagnetic insulating (FMI) state at low temperatures. The FE device with manganite as the channel uses an electric double layer (EDL) as the gate dielectric which can induce large charge density ( $\geq 10^{13}\text{cm}^{-2}$ ) in the channel when a moderate gate bias is applied. The nanostructured nature of the manganite film enhances the field effect by controlling transport within the nano-grain as well as by controlling the depletion layer and the potential barrier at the grain boundaries. We observed a large modulation in the resistance of the film  $\sim \pm 40\%$  at room temperature for a moderate gate bias ( $V_G$ ) of  $\pm 4\text{V}$ , which increased to  $\sim \pm 100\%$  at 100K. The field-effect-induced charges alter the relative fraction of the co-existing phases as well as the characteristic temperatures such as the orthorhombic-orthorhombic ( $O - O'$ ) transition temperature, ferromagnetic transition temperature, and the onset temperature of the low temperature FMI state. The change in the relative fraction of the phases was found to have an exponential dependence on the gate bias. By using the shift in the temperature of the  $O - O'$  transition with gate bias as a reference, we could establish that the change in hole concentration, brought about by the field effect, closely mimics (quantitatively) the change brought about by chemical substitution, including the change in the activation energy of transport in the paramagnetic insulating region.

## 1 Introduction

Control of electronic phases and electrical transport in a strongly correlated oxide film by field effect (FE) using a gate with an electric double layer (EDL) is a topic of considerable current interest<sup>1-4</sup>. The electrolyte used as a gate dielectric forms an EDL at the solid-electrolyte interface, which in turn leads to a large specific gate capacitance that can induce substantial surface charge density ( $\geq 10^{13}/\text{cm}^2$ ) for a moderate applied gate bias<sup>5-7</sup>. This induced surface charge density is orders of magnitude larger than that induced by conventional oxide gate insulators such as  $\text{SiO}_2$ ,  $\text{SrTiO}_3$  for the same bias. Thus, the large induced surface charge density can control the electrical transport of strongly correlated oxides (such as transition metal perovskites), which depends on the carrier density and often with co-existing electronic phases with differing electrical resistivities, as in hole-doped manganites. The native carrier density is very high in the case of transition metal oxides. The induced charge/carrier density by FE with a gate dielectric should be large to produce any observable modulation in these oxides. The large modulation in carrier den-

sity can be achieved using an EDL dielectric. Modulation of the carrier density by FE with a gate dielectric containing an electrolyte or ionic liquid gives rise to various interesting phenomena such as metal-insulator transition<sup>8,9</sup>, superconductivity<sup>1,10</sup> and control of conduction at the grain boundary (GB) region in a functional perovskite<sup>11</sup>. The advantage of FE-induced carrier modulation is that it overcomes the collateral problem of disorder that accompanies carrier modulation by chemical substitution.

In this paper, we show that nanoscopic control of co-existing phases (and through it, control of electronic transport) can be obtained in nanostructured films of functional oxides, such as hole-doped manganites, using an EDL-FET device structure. The control can be bipolar in nature with a positive (negative) gate bias depleting (enhancing) the hole density. We show that the change in the hole density closely mimics the changes that can be brought about by chemical substitution, including structure-related transitions such as the orthorhombic-orthorhombic ( $O - O'$ ) transition seen in manganites. In this report, we bring out the role of gate-bias controlled transport through the grain boundary (GB) region in nanostructured manganite films. The role of the GB in controlling charge transport in manganites is well established,

<sup>a</sup> Dept. of Condensed Matter Physics & Material Sciences, Salt-lake, Kolkata-98, India E-mail: rajibnath.bu@gmail.com \*, & arup@bose.res.in

particularly in the context of its contribution to magnetoresistance<sup>12</sup>. In nanostructured manganites, GB transport takes place across the GB potential barrier by tunneling<sup>13–16</sup>. However, the control of GB barriers by field effect through an applied gate bias has not been adequately addressed in nanostructured manganites. In this paper, we address this issue. We show that the control of GB transport by an applied gate bias occurs in tandem with control of transport within the grain by FE. This in turn leads to substantial control over the co-existing phases. The control of GB transport by FE, though done in the specific context of manganites, can be expected to have a more general application in GB-controlled transport in many nanostructured oxide films.

The work was carried out in a nanostructured film of low-hole-doped manganite ( $\text{La}_{1-x}\text{Ca}_x\text{MnO}_3$ ) with  $x \sim 0.15$  grown on a  $\text{SiO}_2/\text{Si}$  substrate. We have chosen the  $\text{SiO}_2/\text{Si}$  substrate to make the film nanostructured. In a nanostructured film, the FE-induced charge can bring about effective control of transport at two distinct levels. First, it occurs within a grain of the oxide (intra-grain), and second, it can control the potential barrier that forms in the GB region and thus can control inter-grain charge transport. In a recent paper<sup>11</sup>, we have shown that a gate with an EDL dielectric can control the depletion layer in the GB regions.

The choice of low hole-doped manganites  $\text{La}_{1-x}\text{Ca}_x\text{MnO}_3$  (LCMO) is mainly motivated by the fact that it has co-existing electronic phases that vary with temperature. This gives rise to an interesting system where the proposed effects can be observed and investigated. In hole-doped manganites such as LCMO, one can obtain different phases as a function of chemical substitution  $x$ , which in turn controls the hole concentration. LCMO evolves from an orbitally ordered anti-ferromagnetic insulating (AFMI) phase ( $x=0$ ) to a ferromagnetic (FM) metallic phase that occurs for  $x \geq 0.22$ <sup>17–19</sup>. In the intermediate region with  $x \sim 0.15$ , the material shows a ferromagnetic insulating (FMI) phase at low temperature. In this composition range, it shows the coexistence of different phases with different conductivities and different magnetic order that occurs below its ferromagnetic ordering temperature. We have shown that the application of a gate bias that induces large carrier densities can control the relative fraction of co-existing electronic phases, leading to a large change in the transport properties. In a nanostructured film, this effect is enhanced due to the formation of an effective "all-around-gate" by the polymer electrolyte as it flows in the GB region during its solidification. The change in the resistance of the film can be large, and one can obtain bipolar control as the gate bias ( $V_G$ ) is changed from negative to positive. The film resistance is changed by nearly  $\pm 40\%$  at room temperature with a moderate change in the gate bias  $V_G$  by  $\pm 4\text{V}$ , where the negative bias reduces the resistance. At lower temperatures, the effect is significantly enhanced whereby a change of similar magni-

tude in gate bias can change the channel resistance by one order. The applied bias not only changes the resistance, but also affects the temperature range over which co-existing phases are observed and also changes the activation energy for transport in the polaronic paramagnetic insulating state that occurs above the ferromagnetic temperature. This mimics the change in hole concentration brought about by chemical substitution, which we could quantitatively monitor by tracking the change in the  $O - O'$  transition as a function of the applied gate bias  $V_G$ .

## 2 Experiment

The experiment was conducted in a field effect transistor (FET) device configuration with an EDL as the gate dielectric. The device was fabricated with a thin film channel (effective length 1mm and width 300  $\mu\text{m}$ ) of  $\text{La}_{0.85}\text{Ca}_{0.15}\text{MnO}_3$  on  $\text{SiO}_2(300\text{nm})/\text{Si}$  substrate using a stoichiometric target. The thin film channel of thickness  $\approx 10\text{nm}$  was grown by pulsed laser deposition using an excimer laser with the fluence of 1  $\text{J}/\text{cm}^2$  in a 0.1 mbar  $\text{O}_2$  pressure<sup>11</sup>. Atomic force microscopy image of the film (shown in Fig. 1(b)) shows island type growth pattern with bimodal distribution of grain size 3 & 22nm<sup>11</sup>. The source (s) and drain (d) contact pads was made using thermally evaporated Au/Ti. The source and drain pads were protected from the polymer electrolyte by a layer of e-beam resist (PMMA) baked for 3 min at 180°C. The dielectric was applied through a window (opening) in the resist layer on the channel. We used a 10:1 mixture of PEO:  $\text{LiClO}_4$  electrolyte as the gate dielectric<sup>11</sup>. A Cu wire was used as the gate contact. A schematic of the device and the corresponding

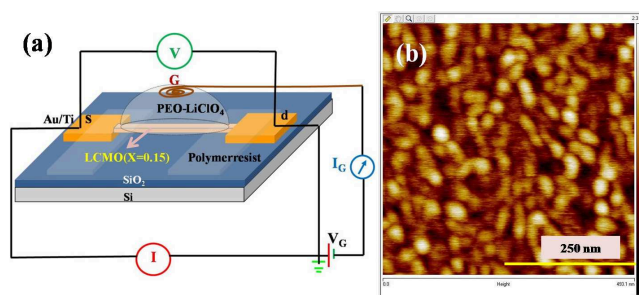


**Fig. 1** (Color online) (a) Schematic diagram of the EDL-FET device with LCMO channel where s, d & G represents the source, drain and gate electrodes. The contact pads at the s and d regions are protected from gate electrolyte by a layer of insulating polymer resist. (b) The AFM topograph of the nanostructured LCMO channel in an area  $\approx 500\text{nm} \times 500\text{nm}$ .

electronic circuit is shown in Fig. 1. We have done the  $I - V$  measurement of the channel with  $V_G=0\text{V}$ <sup>11</sup>. The  $I - V$  curve

is symmetric due to the the identical s and d electrodes having negligible contact resistance. The temperature dependent measurements were carried out in a closed-cycle variable temperature cryostat with a cryo-cooler. The channel resistance  $R$  was measured in a constant current mode (drain current  $I_{DS}$  fixed), and the source-drain voltage ( $V_{DS}$ ) was measured with a source meter usnig the FET configuration shown in Fig. 1(a). The  $R - T$  curves of the channel at different  $V_G$  were measured using a current of  $1 \mu\text{A}$ . Another source-meter was used to apply the gate bias  $V_G$  and detect the gate current  $I_G$  as shown in Fig.1. The gate current ( $I_G$ ) in the steady state is much less than the channel current  $I_{DS}$ , which ensures low leakage at the gate. We have also measured the transient gate current  $I_G(t)$  in response to a step change in gate bias  $V_G$  in order to determine the capacitance of the gate, which we use to measure the amount of induced charge for a given gate bias.

### 3 Modulation of the channel resistance and the characteristic temperatures by Field Effect

The device made with the LCMO  $x=0.15$  channel shows symmetric  $I - V$  curves and the  $I - V$  is linear for low applied bias ( $V_{DS} \leq 0.5\text{V}$ )<sup>11</sup>. To ensure that resistance measurements were carried out within the linear ohmic region, we have measured the resistance of the channel using a low constant current so that the voltage across the source-drain ( $V_{DS}$ ) is less than 0.5 V. The  $R$  vs.  $T$  curves with different gate biases ( $V_G$ ) varying between +4 V to -6 V are shown in Fig. 2. The relative change in the resistance of the channel at room temperature due to the change in the applied  $V_G$  is nearly  $\pm 40\%$ . The change in  $R$  is enhanced at low temperatures. For instance, at  $T = 100\text{K}$ , the channel resistance  $R$  changes from nearly 3 Mohm to 0.2 Mohm with increasing  $V_G$  from +4 V to -6 V. The evolution of channel resistance as a function of gate bias  $V_G$  is also accompanied by a shift in some of the characteristic temperatures, indicating a transformation between the different co-existing phases in the film. This can be appreciated from a change in the shape of the  $R - T$  curve with different  $V_G$ . To identify these temperatures clearly, we have taken the derivatives of the  $R - T$  curves as shown in Fig. 3. In the figure, we plot  $\frac{d(\ln RT^{-1})}{dT^{-1}}$  as a function of  $T$  at  $V_G=0\text{V}$  and at a few representative  $V_G$  values. The derivative curve accentuates the three characteristic temperatures clearly as a deviation from a smooth temperature variation. These temperatures are marked in Fig. 3. However, the identity of these characteristic temperatures cannot be inferred from the  $R - T$  curve alone as doing so it requires the use of a multitude of other techniques, which are difficult to directly perform on a thin film in the FET configuration. Therefore, we have used the known phase diagram of LCMO (as a function of  $x$ )<sup>17-19</sup>, to identify these temperatures from the derivative curve at  $V_G = 0\text{V}$ .

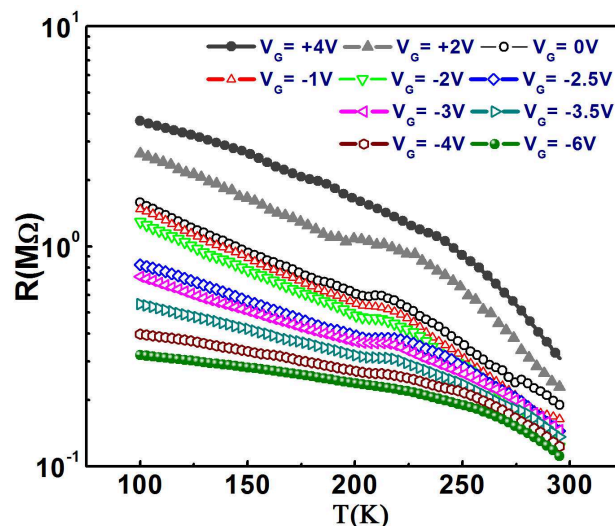
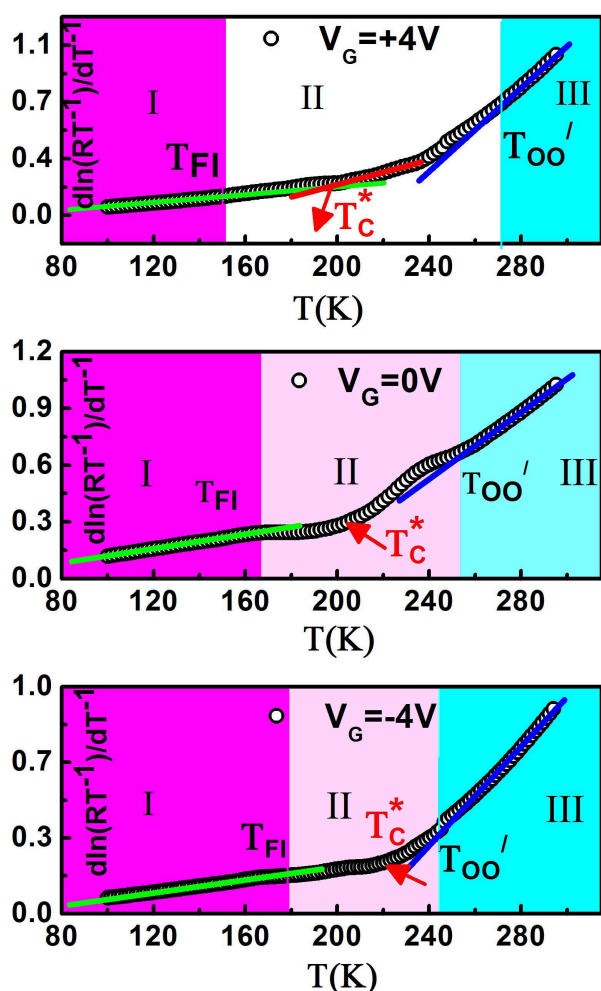


Fig. 2 (Color online)  $R - T$  curves of the channel with different gate bias. Positive gate bias enhances  $R$  while negative bias suppresses  $R$ .

From the evolution of the derivative curves, we track how these temperatures change with  $V_G$ . The co-existence of different phases in low-doped manganites like LCMO  $x=0.15$  are known from past investigations<sup>17-19</sup>. These phase coexistence can be perturbed by temperature or by external stimuli like pressure in our case it is the charge induction the channel using electrolytic gate. The gating actually controls the intra-graining (by modulating the carriers) as well as the inter-grain conduction by modulating the GB potential barrier<sup>11</sup> of the channel. In LCMO  $x=0.15$ , there are 3 regions (regions I, II, and III) that can be identified. Region I is a low-temperature ferromagnetic insulating state (FMI), the onset of which is marked by the temperature  $T_{FI}$ , which in turn also changes with hole concentration. Region II is a predominantly mixed phase region with a co-existing low resistance FM phase (which may be a high resistive metallic phase having a shallow  $T$  dependence and a high-resistance insulating phase. There is also a paramagnetic to ferromagnetic transition that shows up as a change in the slope of the  $R - T$  curve. This we mark as the temperature  $T_C^*$  (Note: we distinguish this from the ferromagnetic transition temperature  $T_C$ , which is determined by magnetic measurements. The temperatures  $T_C^*$  and  $T_C$  may be close but not necessarily the same. However, for our film, for  $V_G = 0$ ,  $T_C^*$  determined from the derivative curve matches with the  $T_C$  value, as determined by magnetic measurements). In region III, the system is in a paramagnetic insulating (PI) state with an orthorhombic phase ( $O$  phase). It undergoes structural distortion due to the onset of cooperative Jahn-Teller (JT) transition and assumes a distorted orthorhombic structure with rotated octahedra marked as  $O'$  phase (Note:

resistivity data taken on single crystals also show this transition as a change in the slope at the  $OO'$  transition determined crystallographically<sup>20,21</sup>). The transition temperature marked as  $T_{OO'}$  in Fig. 3 is an important marker for the hole concentration as it is suppressed at increasing hole concentrations<sup>21</sup>. The characteristic temperatures obtained from the  $\frac{d(\ln RT^{-1})}{d(T^{-1})}$



**Fig. 3** (Color online) The characteristics temperatures of the LCMO channel are marked as determined from transport data by plotting normalized  $\frac{d(\ln RT^{-1})}{dT^{-1}}$  vs.  $T$  at  $V_G = +4V$ ,  $0V$  and  $-4V$  respectively. Color boundaries indicate different characteristic regions with their temperatures  $T_{FI}$  (color boundary of region I) and  $T_{OO'}$  (color boundary of region III). Red arrow represents the position of  $T_C^*$ .

vs.  $T$  curve as shown in Fig. 3 at  $V_G = 0$  matches well with reported data for LCMO  $x=0.15$ <sup>17–19</sup>. Application of  $V_G$  of either polarity shifts these temperatures. In Fig. 4, we show the evolution of the three temperatures ( $T_{OO'}$ ,  $T_C^*$  and  $T_{FI}$ ) as a function of the gate bias. All the three temperatures show

substantial change on application of a moderate gate bias. Importantly, the change is bipolar with a positive (negative)  $V_G$  that leads to hole depletion (enhancement) depressing (raising)  $T_C^*$  and raising (depressing)  $T_{OO'}$ . We show below that the changes brought about by the gate-induced charges (FE-induced charges) mimic the changes that one would expect by a change in hole concentration ( $\delta x$ ) in  $\text{La}_{1-x}\text{Ca}_x\text{MnO}_3$  brought about by chemical substitution<sup>17–19</sup>. The variation in the characteristic temperatures with gate bias is closely related to the change in the relative fraction of the co-existing phases which we will discuss in later sections. The observation that one can tune the temperature  $T_{FI}$  as well as  $T_{OO'}$  by an applied gate bias is new and is a direct manifestation of the fact that the FE-induced charges can change the hole concentration in a manner similar to that achieved by chemical substitution.

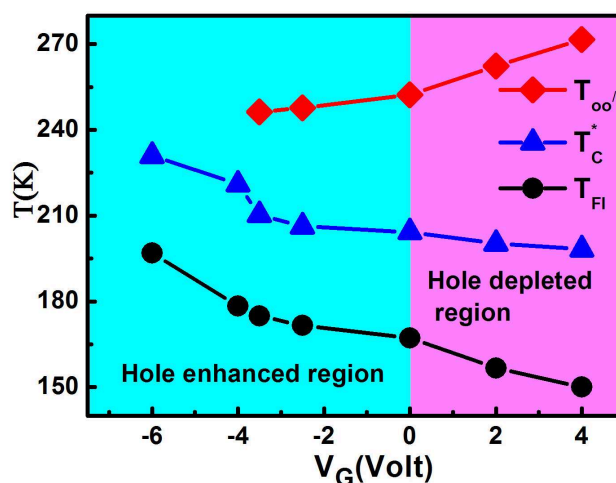


**Fig. 4** (Color online) Variation of characteristics temperatures  $T_{OO'}$ ,  $T_C^*$  and  $T_{FI}$  as a function of gate bias. The characteristics temperatures are obtained from Fig. 3

#### 4 The Field effect and induced charge in channel

The observed bipolar modulation of the channel resistance arises from the modulation of carrier density due to the application of a finite gate bias. The electric field due to the formation of an EDL near the electrolyte–channel interface affects the carrier concentration in the channel, mostly over a length scale of the order of the Debye length from the surface<sup>22,23</sup>. We have calculated the Debye length ( $\lambda_D$ ) of the sample using the equation  $\lambda_D = \sqrt{\frac{\epsilon_r \epsilon_0 \kappa_B T}{n_{3D} e^2}}$ , where  $\epsilon_0$  is the permittivity of free space,  $\epsilon_r$  is the dielectric constant of the material,  $\kappa_B$  is the Boltzmann constant,  $e$  is the electronic charge and  $n_{3D}$  is

the volume carrier density in the channel. We obtain  $\lambda_D \approx 4$  nm at  $T=300\text{K}$  using the value of  $\epsilon_0$ ,  $n_{3D} \approx 10^{21}/\text{cm}^3$  and  $\epsilon_r \approx 100$  (for LCMO)<sup>24</sup>. The estimated  $\lambda_D$  is comparable to the average grain size ( $\approx 3\text{nm}$ ) of the film, and the film thickness, though somewhat large, is also comparable ( $\approx 2.5\lambda_D$ ) to this length scale. Since the electrolyte flows around the grains during its solidification, we may assume that the entire thickness of the channel is affected more or less uniformly by the field-induced charge, and an effective carrier density modulation can be achieved by the applied gate bias  $V_G$ . In Fig. 5, we schematically show the effect of the gate bias on the channel-electrolyte interface, which modulates the carrier as well as the GB potential barrier.

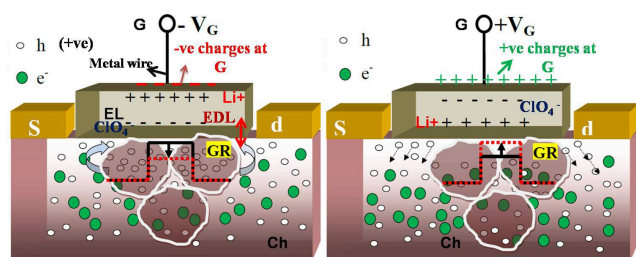


**Fig. 5** (Color online) Schematic diagram of (a) effect of  $-V_G$  within the channel; s,d & G are source, drain & Gate electrodes. EL & Ch represents Electrolyte and the channel. h, e, and GR represents holes, electrons and grains and black rectangular well represent GB potential barrier at  $V_G=0\text{V}$ . Red (lower) rectangular well represent the barrier potential at GB at  $-V_G$  (b) Effect of  $+V_G$  within the channel. Red rectangular well represent the barrier potential at GB at  $+V_G$ .

## 5 A quantitative comparison of changes in hole concentrations achieved by gate induced FE and that achieved by chemical doping ( $\delta x$ )

In the previous section, we observed that a moderate gate bias can tune  $R$ , its temperature dependence, and can also substantially affect the characteristic temperatures ( $T_{OO'}$ ,  $T_C^*$  and  $T_{FI}$ ). In this section, we will quantitatively compare the changes brought about by the gate-induced carriers with that expected from chemical doping ( $\delta x$ ). We estimate the change in hole concentration ( $\delta x$ ) from the shift in  $T_{OO'}$ , as achieved by the field effect, and compare that with the change in hole concentration calculated from the gate bias and specific gate capacitance that gives the electrostatically induced charge density. An enhanced hole concentration suppresses the  $T_{OO'}$ <sup>17–19,21</sup>. Since the change in  $T_{OO'}$  as a function of  $x$  (brought about by chemical substitution) is well established, its change with gate bias can thus be used as a calibrated measure of the effective change in hole concentration  $\delta x$  due to  $V_G$ .

In our previously reported experiment, we measured the transient gate current  $I_G(t)$  in response to a step change in the gate bias  $V_G$ <sup>11</sup>. Analysis of the transient gate current has been used to obtain the gate capacitance ( $C_g$ ) from the charging time constant ( $R_g C_g$ ), where  $R_g$  is the gate resistance through which the gate capacitance charges. From the measured  $C_g$ , we obtain a specific gate capacitance  $\approx 1.6\mu\text{F}/\text{cm}^2$ . We estimate an induced surface charge density of  $1 \times 10^{13}/\text{cm}^2$  for a gate bias of 1V. Using the value  $\lambda_D \approx 4$  nm at  $T=300\text{K}$  and the assumption that induced carriers can affect the carrier density in the channel over a depth roughly equal to the Debye length from the surface  $\approx \lambda_D$ , we find a volume charge density of  $\approx 0.5 \times 10^{19}/\text{cm}^3$  for a gate bias change of 1V. From the formula unit volume of  $\approx 60 \text{ \AA}^3$  for LCMO, we find the induced carrier density causes a change of  $\delta x \approx \mp 0.0013$  /formula unit for  $V_G = \pm 1\text{V}$ . To distinguish this  $\delta x$ , obtained from the electrostatic method, from that obtained by chemical substitution, we call it  $\delta x_e$  to mean that this has been brought upon by an electrostatic effect. In Figure 6, we show  $\delta x_e$  as a function of  $V_G$ . This shows the change in hole concentration expected from a gate-induced field effect.

We have calculated the modulation of  $\delta x$  with a variation of  $T_{OO'}$  from the known linear variation of  $T_{OO'}$  with  $x$  in  $\text{La}_{1-x}\text{Ca}_x\text{MnO}_3$  when  $x$  is changed by chemical substitution, as documented in the phase diagram of  $\text{La}_{1-x}\text{Ca}_x\text{MnO}_3$ <sup>17–19</sup>. From the data, we find that a lowering of 1K in  $T_{OO'}$  occurs due to an enhancement of  $\delta x \approx 3 \times 10^{-4}$ . From Fig. 4, we could thus calculate the variation of  $\delta x$  as a function of  $\pm V_G$ . In Fig. 6, we have shown the variation of  $\delta x$  with  $V_G$  along with  $\delta x_e$ . From Fig. 6, it can be seen that the estimated values

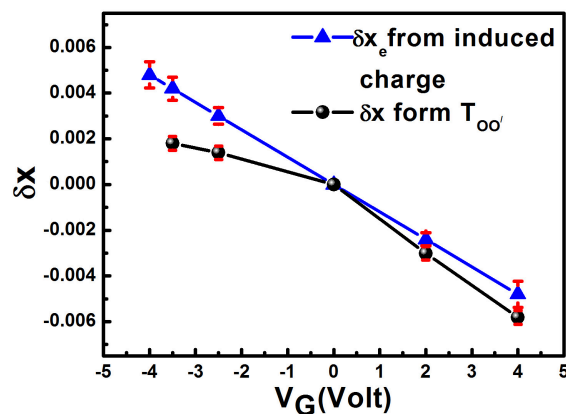


**Fig. 6** (Color online) Variation of  $\delta x$  and  $\delta x_e$  with different  $V_G$  calculated from induced charge due to field effect ( $\delta x_e$ ) and from the change in  $T_{OO'}$  ( $\delta x$ ).

of  $\delta x$  from  $T_{OO'}$  and  $\delta x_e$  derived from the FE-induced charge are nearly the same in the positive gate voltage region ( $+V_G$ ). It is of similar order, but somewhat different in magnitude in the

negative gate voltage ( $-V_G$ ) region. It is indeed gratifying that  $\delta x$  and  $\delta x_e$ , though estimated from two independent methods, give similar values. It establishes that the change in hole concentration as a result of the field effect (using the EDL dielectric) is predominantly an electrostatic effect. There is a difference between  $\delta x$  &  $\delta x_e$  in the negative gate bias region, where we find that  $\delta x < \delta x_e$ . This implies that hole accumulation within a grain due to the field effect is less than that expected from a simple electrostatic effect. This difference likely arises from the fact that parts of the induced holes (being majority carriers) compensate the heavily depleted GB region. In such nanostructured films, the GB region being strongly depleted of majority carriers, forms a depletion region<sup>11</sup>. A part of the FE-induced charge leads to lowering of the GB potential barrier and narrowing of the depletion layer (schematically shown in Fig. 5). For a positive gate bias, where the hole concentration is reduced with gate bias, the GB region gets further depleted (schematically shown in Fig. 5). This makes the value of  $\delta x$  closer to that of  $\delta x_e$  but  $|\delta x|$  is somewhat larger than  $|\delta x_e|$ .

## 6 Dependence of the activation energy of transport on gate bias.

In the temperature range  $T > T_C^*$ , the charge transport is strongly activated with an activation energy  $E_a$ . The charge transport within a grain is polaronic in nature and the activation of transport has a polaronic origin. In manganites,  $E_a$  can be affected by the structural changes (due to external pressure), presence of the GB potential barrier as well as defects present in the system<sup>25–27</sup>. Here, we observed that the FE-induced charges & modulation of the GB potential barrier plays an important role to change the  $E_a$  of the channel. The change in  $E_a$  with gate bias  $V_G$  can be compared qualitatively to the change in  $E_a$  that can arise from hole doping by substitution (change in  $x$ )<sup>20</sup>. The applied gate bias can lead to modulation of both the polaronic contribution to  $E_a$  as well as that arising from the GB barrier. In the temperature region of interest ( $T > T_C^*$  at  $V_G = 0$  and negative  $V_G$ ), owing to the lowering of the GB barrier by the induced hole, it is expected that the activation energy  $E_a$  will predominantly be of polaronic origin following the equation  $R = R_0 T \exp(\frac{E_a}{k_B T})$ <sup>20</sup>. It has been known from past studies on single crystals<sup>20</sup> that the activation energy  $E_a$  is suppressed by enhancement of  $x$  (enhancement of hole doping). Thus the reduction in  $E_a$  with applied negative gate bias can be understood. For positive gate bias, where the hole density is depleted, one would expect  $E_a$  to increase. However, the magnitude of change of  $E_a$  in this region is very steep and is more than what one would expect from a change in hole density alone<sup>20</sup>. It is likely that the steep change in  $E_a$  is a reflection of the enhancement of the GB barrier that can occur due to a strongly depleted GB region.

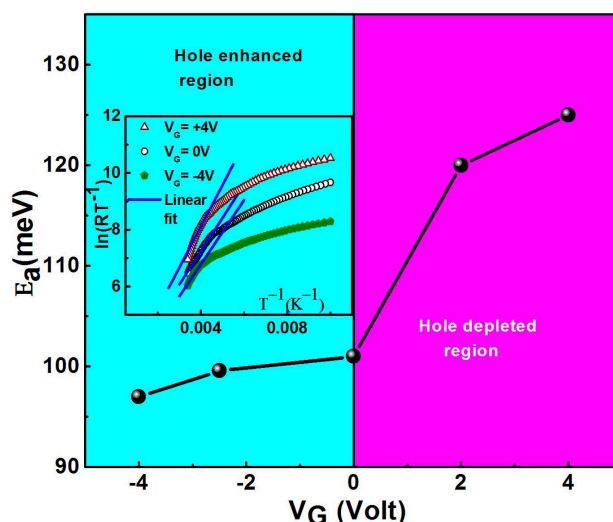


**Fig. 7** (Color online) Variation of  $E_a$  with different  $V_G$ . The inset shows adiabatic polaronic fit to the  $R-T$  data at  $V_G = +4V, 0V$  &  $-4V$  respectively from which  $E_a$  are determined at different  $V_G$ .

## 7 Control of coexisting electronic phases by gate bias

The evolution of channel resistance  $R$  as a function of temperature  $T$  as well as gate bias  $V_G$  can be phenomenologically explained as arising from the evolution of the relative fraction ( $f$ ) of the two co-existing phases in the channel. The transport in regions I and II takes place predominantly through the two co-existing phases: one, a high-resistance insulating phase (resistance denoted by  $R_{ins}$ ), and the other, a low-resistance 'marginally' metallic phase, whose resistance is denoted by  $R_m$  (we call it metallic for reference purposes only). It can be a high resistive metallic phase (having higher resistance than the normal metals) with relatively lower resistance than the insulating phase. Changes in  $T$  and  $V_G$  alter the relative fraction  $f$  of the two co-existing phases. Thus the change in  $f$  can phenomenologically describe the change in  $R$  as a function of  $T$  and  $V_G$ . The transport and magnetic properties in low-hole-doped manganites  $x \leq 0.2$  have been explained using such co-existing phases as stated before<sup>19</sup>.

A change in the intragrain hole concentration will alter the relative fraction of the coexisting phases; however, the observed effective  $f$  will also depend on the conductivity of the GB region. For a negative gate bias that reduces the GB potential barrier owing to an increase in the number of holes, one would see an enhancement of the effective  $f$  over and above that expected from changes within a grain alone. Similarly, a gate-bias-induced enhancement of GB potential that occurs at positive  $V_G$  will contribute to a reduction of the effective  $f$ .

Thus, in the nanostructured film, the potential barrier at the GB will affect the effective  $f$ .

We obtain an estimate of  $f$  from a simple 2-phase model for conduction. In the presence of two such phases, the channel resistance ( $R$ ) can be expressed as

$$\frac{1}{R} = \frac{(1-f)}{R_{ins}} + \frac{f}{R_m}, 0 \leq f \leq 1, \quad (1)$$

We have assumed  $R_{ins}(T)$  as the resistance of the channel at  $V_G = +4V$ . The rationale for this assumption is that hole depletion at positive bias converts the channel into a high-resistance insulating phase with a metallic fraction  $f \rightarrow 0$  along with the highly depleted GB region with an enhanced GB barrier.  $R_m(T)$  is taken as the resistance of the channel at  $V_G = -6V$ , where we assume that the entire channel, by the enhancement of hole concentration, has only the 'metallic' phase ( $f \rightarrow 1$ ) with a reduction in the depletion region and the GB barrier potential. From equation 1, we obtained  $f$  as a function of  $T$  for different gate bias ( $V_G$ ). We have limited our analysis to  $T < T_{OO}$  where we have the mixed-phase region. In Fig. 8, we have plotted the metallic fraction ( $f$ ) vs.  $T$  curve for different  $V_G$ . Fraction  $f$  can be written as  $f(T, V_G)$  since it is a function of both  $T$  and  $V_G$  as seen in Fig. 8. At  $T \leq$

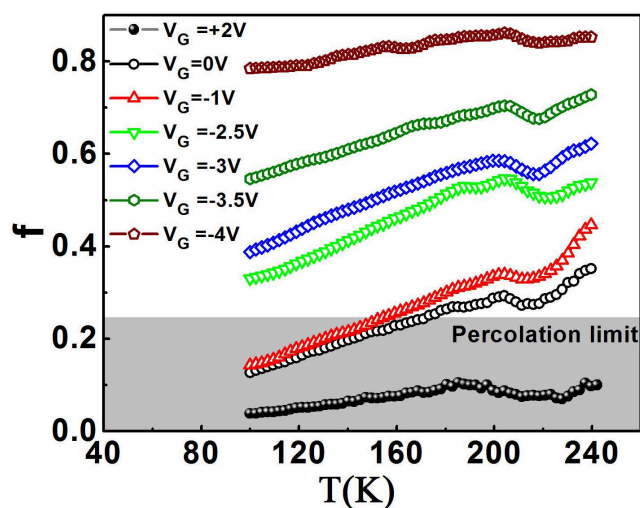


**Fig. 8** (Color online) Temperature dependence of  $f$  with different  $V_G$ .

240K, for all gate bias values,  $f(T, V_G)$  decreases on cooling due to the activated nature of the transport in the channel as well as due to the barrier in the GB region. However, the temperature dependence becomes less steep as  $V_G$  becomes more negative and  $f$  increases. The temperature dependence is more steeper when  $V_G > 0$ , which depletes the hole density in the channel, thus enhancing the insulating fraction of the coexisting phases. A negative  $V_G$ , which leads to the

accumulation of more holes in the channel, in turn, leads to a larger  $f(T, V_G) \rightarrow 1$ , and the temperature dependence of  $f(T, V_G)$  also becomes less steep due to the predominance of the metallic fraction. For  $V_G \approx -3V$  and beyond, it is more or less  $T$  independent. For positive  $V_G (\geq 2V)$ , the metallic fraction  $f(T, V_G)$  is below the percolation limit for volume percolation<sup>28</sup> ( $f_P = 0.25$ ), and the insulating phase makes a predominant contribution to the transport as  $f(T, V_G) < f_P$ .  $f(T, V_G)$  depends on both  $T$  and the gate bias  $V_G$ . The explicit dependence of  $f(T, V_G)$  on  $T$  is given by  $f_0(T)$ , which gives the temperature variation for zero bias. The scaled quantity  $f(T, V_G)/f_0$  would thus show an explicit dependence of the fraction  $f$  on the applied gate bias. If we consider the scenario wherein the gate bias control of  $f$  predominantly occurs due to control of the GB conductivity by  $V_G$ , then one would expect that  $f(T, V_G)/f_0$  is directly proportional to the GB conductance  $G_{GB}$ . It has been established through experimentation on GB conductance that it is controlled primarily by tunneling at the GB<sup>16,29,30</sup>. The tunneling takes

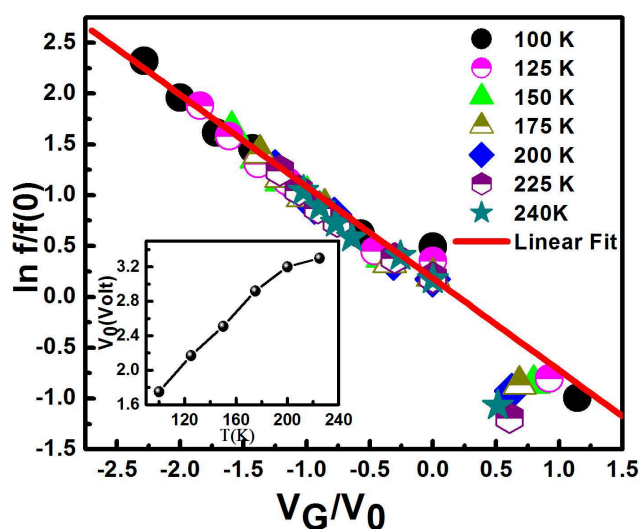


**Fig. 9** (Color online) The field dependence of the scaled  $f(V, T)/f_0$  with  $V_G/V_0$ . The inset shows the  $T$  dependence of  $V_0(T)$ .

place through the depletion layer of thickness  $t$ , which is given by  $t = \sqrt{\frac{2\epsilon_0\epsilon_r\phi_{GB}}{e^2n_{3D}}}$ , where  $\phi_{GB}$  is the GB potential barrier.  $G_{GB}$  is  $\propto \exp(-\chi.t)$ , where the inverse tunneling length  $\chi = \sqrt{\frac{2m\phi_{GB}}{h^2}}$ . Thus  $G_{GB}$  will be determined by the  $\chi t$  product, where  $\chi t = \sqrt{\frac{4m\epsilon_0\epsilon_r}{e^2h^2n_{3D}}}\phi_{GB}$ . The application of the gate bias will change both the barrier  $\phi_{GB}$  and  $n_{3D}$  leading to a change in  $G_{GB}$  and thus  $f(T, V_G)/f_0$ . The GB barrier  $\phi_{GB}$  has an inverse dependence on gate bias  $V_{GB}$ , as established

through such studies on polycrystalline semiconductors<sup>31</sup>. Using the above discussion, we argue that  $f(T, V_G)/f_0$  will have an exponential dependence on  $V_G$  and we can write the dependence of  $f(T, V_G)$  on  $T$  and  $V_G$  as :

$$f = f_0(T) \exp\left(-\frac{V_G}{V_0}\right), \quad (2)$$

where  $f_0(T)$  describes the  $T$  dependent evaluation of  $f$  at  $V_G=0$  as stated before. The scaling voltage  $V_0$  may itself have a weak  $T$  dependence because it can have a dependence on  $\epsilon_r$  as well as on  $n_{3D}$ , both of which have a  $T$  dependence (Note: The  $T$  dependence of  $n_{3D}$  occurs due to dependence of  $\lambda_D$  on  $\epsilon_r$ ). To check the validity of the above relation, we plot a scaled graph where  $\ln(f(T, V_G)/f_0)$  is plotted vs.  $V_G/V_0$ . We find that all the data for  $f$  can be merged onto the scaled curve that has a single parameter  $V_0$ . The values of  $V_0$  at each  $T$  needed to merge all the data onto a single curve are shown in the inset. Fig. 9 establishes the exponential dependence of fraction  $f$  on the gate bias and it shows that the phase control is predominantly brought about by the control of the potential barrier  $\phi_{GB}$ . The parameter  $V_0(T)$  has a linear dependence on  $T$ .

## 8 Conclusions

In conclusion, we have shown that by using a gate dielectric with an EDL, it is possible to control the relative fraction of coexisting phases in film of low-hole doped  $\text{La}_{1-x}\text{Ca}_x\text{MnO}_3$  with  $x=0.15$ . The FE induced charges not only change the resistance of the film (channel in the FET device), it also changes the relative fraction  $f$  of the co-existing phases as well as the characteristic temperatures  $T_{OO'}$ ,  $T_C^*$  and  $T_{FI}$ . The substantial control of the gate bias on the co-existing phases as well as on the charge transport in such films has been enabled by the effect of the gate bias on  $\phi_{GB}$  which in effect controls the GB transport. We have shown that the exponential control of the gate bias  $V_G$  on  $f$  originates from the predominant control of  $\phi_{GB}$  by  $V_G$ . We have also shown that the change brought about by the FE closely mimics (quantitatively) that obtained by chemical substitution. One of the important observations in this study is that the FE can change the  $O - O'$  transition temperature, which shows a characteristic feature at  $T_{OO'}$ , identifiable from the resistance data. While  $T_{OO'}$  gets suppressed on hole accumulation, the ferromagnetic transition temperature  $T_C^*$  is enhanced. Though we could not establish the enhancement in  $T_C^*$  with applied gate bias through direct magnetic measurements, it is intriguing that such a moderate gate bias (with EDL dielectric) can lead to appreciable hole density enhancement, such that the onset of the FM transition can be so much

enhanced. This behavior compares very well to the phase-diagram of  $\text{La}_{1-x}\text{Ca}_x\text{MnO}_3$  when  $x$  is changed by substitution.

## 9 Acknowledgments

The authors acknowledge the financial support from the Department of Science and Technology, Government of India as a sponsored project as a Unit for Nanoscience. R.N. acknowledges the support from CSIR as a Senior Research Fellowship. A.K.R. acknowledges J.C. Bose Fellowship for additional support.

## References

- 1 K. U. et al., *Nature Mater.*, 2008, **7**, 855–858.
- 2 Y. Lee, C. Clement, J. Hellerstedt, L. K. Joseph Kinney, X. Leng, S. D. Snyder and A. M. Goldman, *Phys. Rev. Lett.*, 2011, **106**, 136809.
- 3 M. Lee, J. R. Williams, S. Zhang, C. D. Frisbie and D. Goldhaber-Gordon, *Phys. Rev. Lett.*, 2011, **107**, 256601.
- 4 T. Hatano, Y. Ogimoto, N. Ogawa, M. Nakano, S. Ono, Y. Tomioka, K. Miyano, Y. Iwasa and Y. Tokura, *Sci. Rep.*, 2013, **3**, 2904.
- 5 A. T. A. O. M. K. Hongtao Yuan, Hidekazu Shimotani and Y. Iwasa, *Adv. Funct. Mater.*, 2009, **19**, 1046.
- 6 H. Yuan, H. Shimotani, J. Ye, S. Yoon, H. Aliah, A. Tsukazaki, M. Kawasaki and Y. Iwasa, *J. AM. CHEM. SOC.*, 2010, **132**, 18403.
- 7 H. Du, X. Lin, Z. Xu1 and D. Chu1, *J Mater. Sci*, 2015, DOI 10.1007/s10853-015-9121-y.
- 8 K. Ueno, S. Nakamura, H. Shimotani, H. T. Yuan, N. Kimura, T. Nojima, H. Aoki, Y. Iwasa and M. Kawasaki, *Nature Nanotech.*, 2011, **6**, 408.
- 9 A. S. Dhoot, C. Israel, X. Moya, N. D. Mathur and R. H. Friend, *Phys.Rev.Lett.*, 2009, **102**, 136402.
- 10 H. Shimotani, H. Asanuma, A. Tsukazaki, A. Ohtomo, M. Kawasaki and Y. Iwasa, *Appl. Phys. Lett.*, 2007, **91**, 082106.
- 11 R. Nath and A. K. Raychaudhuri, *Appl. Phys. Lett.*, 2014, **104**, 083515.
- 12 R. Mahesh, R. Mahendiran, A. K. Raychaudhuri and C. N. R. Rao, *Appl. Phys. Lett.*, 1996, **68**, 2291.
- 13 B. Ghosh, S. Kar, L. K. Brar and A. K. Raychaudhuri, *J. Appl. Phys.*, 2005, **98**, 094302.
- 14 M. A. Paranjape, K. S. Shankar and A. K. Raychaudhuri, *J. Phys. D.*, 2005, **38**, 3674.
- 15 T. Sarkar, M. V. Kamalakar and A. K. Raychaudhuri, *New. J. Phys.*, 2012, **14**, 033026.
- 16 J. Klein, C. Hofener, S. Uhlenbruck, L. Alff, B. Buchner and R. Gross, *Europhys. Lett.*, 1999, **47**, 371.
- 17 P. Schiffer, A. P. Ramirez, W. Bao and S.-W. Cheong, *Phys. Rev. Lett.*, 1995, **75**, 3336.

- 
- 18 R. Mahendiran, S. Tiwary, A. Raychaudhuri, T. Ramakrishnan, R. Mahesh, N. Rangavittal and C. Rao, *Phys. Rev. B.*, 1996, **53**, 3348.
  - 19 E. Dagotto, H. Takashi and A. Moreo, *Phys. Rep.*, 2001, **344**, 1–153.
  - 20 H. Jain, A. Raychaudhuri, Y. M. Mukovskii and D. Shulyatev, *Solid state communications*, 2006, **138**, 318.
  - 21 C. Ritter, M. R. Ibarra, J. M. D. Teresa, P. A. Algarabel, C. Marquina, J. Blasco, J. Garcia, S. Oseroff and S. W. Cheong, *Phys. Rev. B*, 1997, **56**, 8902.
  - 22 Y. Zhou and S. Ramanathan, *Critical Reviews in Solid State and Materials Sciences*, 2013, **38**, 286.
  - 23 C. H. Ahn, J. M. Triscone and J. Mannhart, *Nature*, 2003, **424**, 1015.
  - 24 J. L. Cohn, M. Peterca and J. J. Neumeier, *Phys. Rev. B*, 2004, **70**, 214433.
  - 25 R. Thiyagarajan, N. Manivannan, S. Arumugam, S. E. Muthu, N. R. Tamilselvan, C. Sekar, H. Yoshino, K. Murata, M. O. Apostu, R. Suryanarayanan and A. Revcolevschi, *J. Phys.: Condens. Matter*, 2012, **24**, 136002.
  - 26 K. D. Chandrasekhar, A. K. Das, C. Mitra and A. Venimadhav, *J. Phys.: Condens. Matter*, 2012, **24**, 495901.
  - 27 H. Rahmouni, M. Smari, B. Cherif, E. Dhahrib and K. Khirounia, *Dalton Trans.*, 2015, **44**, 10457.
  - 28 Q. Xue, *Physica B*, 2003, **325**, 195.
  - 29 N. Khare, U. Moharil, A. Gupta, A. Raychaudhuri and R. P. SP Pai, *Appl. phys. lett.*, 2002, **81**, 325.
  - 30 M. Paranjape, J. Mitra, A. Raychaudhuri, N. Todd, N. Mathur and M. Blamire, *Phys. Rev. B.*, 2003, **68**, 144409.
  - 31 T. Serikawa, S. A. Okamoto and S. Suyama, *IEEE Trans ED.*, 1984, **34**, 321.